NASA Technical Memorandum 81615

Effect of a Semi-Annular Thermal Acoustic Shield on Jet Exhaust Noise

J. Goodykoontz
Lewis Research Center
Cleveland, Ohio

Prepared for the
One-hundredth Meeting of the Acoustical Society of America
Los Angeles, California, November 17-21, 1980

NASA

EFFECT OF A SEMI-ANNULAR THERMAL ACOUSTIC SHIELD ON JET EXHAUST NOISE

by J. Goodykoontz

National Aeronautics and Space Administration
Lewis Research Center
Cleveland, Ohio 44135

ABSTRACT

Previous experimental studies have shown that reductions in jet exhaust noise were obtained by the use of an annular thermal acoustic shield consisting of a high temperature, low velocity gas stream surrounding a high velocity central jet exhaust. The reductions obtained with the annular shield appear to be limited by multiple reflections. It has been hypothesized that a semi-annular shield would provide greater noise reductions by eliminating the multiple reflections. The present work consisted of an exploratory study to investigate the effect of a semi-annular shield on jet exhaust noise with the rationale that such a configuration would eliminate or reduce the multiple reflection mechanism. Noise measurements for a 10 cm conical nozzle with a semi-annular acoustic shield are presented in terms of lossless free field data at various angular locations with respect to the nozzle. Measurements were made on both the shielded and unshielded sides of the nozzle. The results are presented parametrically, showing the effects of various shield and central system velocities and temperatures. Selected results are scaled up to a typical full scale engine size to determine the perceived noise level reductions.

INTRODUCTION

In order to meet proposed lower future aircraft noise level goals to satisfy community demands, continued research and development activity is needed to find alternative methods for additional noise suppression. The need is especially critical for supersonic cruise civil aircraft and the increased jet noise levels associated with this type of aircraft.

Previous experimental model studies (Refs. 1 to 8) showed that a reduction in sound levels can be obtained by employing an impedance changing medium in the radiation path between a noise source and measuring station. The impedance changing media included an acetylene flame (Ref. 2), a helium gas stream (Ref. 3), and a fluid thermal acoustic shield or high temperature low velocity air stream (Refs. 4 to 8). The thermal acoustic shield concept appears to be applicable to engine jet exhaust noise suppression. The studies indicated that attenuation increases with an increase in frequency and that a reduction in jet mixing noise levels occurred at large directivity angles, referenced to the upstream jet axis. The reduction in high frequency noise is an attractive consequence since suppressor nozzles, which are dominant in high frequency noise emission, are the most likely candidates for future civil supersonic cruise aircraft (Ref. 9). Also, since jet exhaust noise peaks in the rear quadrant at large directivity angles, the possibility of reducing the peak noise warrants investigation.

Results presented in Ref. 7 for a conventional bypass nozzle showed that a considerable reduction in spectral sound pressure levels occurred, compared to the levels of the central core nozzle alone, when the outer stream was heated. The reduction, in part, was believed to be caused by the shielding effects of the outer jet. In Ref. 4 it was suggested the use of a semi-annular thermal acoustic shield for an engine nozzle application to redirect the noise from the main propulsion nozzle. This scheme would possibly eliminate or minimize the multiple reflections inherent in a complete annular arrangement.

In this paper, the noise reduction benefits of the semi-annular thermal acoustic shield concept were determined experimentally. The effort was exploratory in that only a limited range of flow conditions for one nozzle/shield configuration was studied at model scale. A coaxial nozzle with one half of the outer flow passage blocked off was used as the test configuration. The conical, or core, nozzle flow was varied from a pressure ratio of 1.6 to 2.2 and temperature was varied from 290 to 1089 K. Shield flow velocity was held nominally constant at 220 m/sec with the temperatures varying from 700 to 922 K. The measured data are presented in terms of directivity patterns and sound pressure level spectra to show the effect of shield flow on the noise characteristics of the conical nozzle.

APPARATUS AND PROCEDURE

Facility

A photograph of the flow facility used for the acoustic experiments is shown in Fig. 1. A common unheated laboratory air source supplied flow for two parallel flow lines, one line for the inner nozzle and the other for the outer shielding flow nozzle. Each flow line had its own air and fuel flow control and flow measuring systems. The air in each line could be heated by jet engine combustors. Mufflers in each line attenuated flow control valve noise and internal combustion noise. The system was designed for maximum nozzle exhaust temperatures of 1100 K and nozzle pressure ratios of 3.0 in both the inner and outer stream flow lines.

A sideline microphone array was used for the tests described herein. The microphones (0.635 cm) were placed at a constant 5.0 meter distance from and parallel to the nozzle axis, as shown in Fig. 2. The microphone grids were removed to improve high frequency performance. The ground plane of the test area was asphalt and concrete covered with 15.25 cm thick foam rubber blankets.

Test Nozzle

A schematic of the test nozzle configuration is shown in Fig. 3. An existing coplanar coaxial nozzle was modified to serve as the experimental model for the thermal acoustic shield tests (Ref. 10). The core or conical nozzle had a 10.1 cm inner diameter at the exit plane and the unmodified coaxial nozzle had an area ratio (outer to inner) of 1.4. The annular gap was 2.54 cm. One half of the outer nozzle flow passage was blocked off at the exit plane by a series of 0.32 cm thick overlapping steel plates. The blocking plates were overlapped to account for differential thermal expansion between the two nozzles during the tests and thereby to minimize flow

leakage. The outer wall of the inner nozzle was coated with a ceramic material to minimize heat transfer between the two streams during operation. The interior of the upstream portion of the inner nozzle supply line was also lined with insulating material.

Procedure

All tests were conducted with steady-state flow conditions for given nozzle total pressures and temperatures. Upstream plenum chamber total pressures and total temperatures were used to calculate nozzle exhaust velocities assuming ideal expansion to atmospheric conditions. Nozzle throat static temperatures were calculated from the measured total temperatures after correcting the total temperature for thermocouple radiation heat loss.

An on-line analysis of the noise signal from each microphone in succession was performed. One-third octave band sound pressure level spectra were digitally recorded on magnetic tape and subsequently processed to give lossless data at the particular microphone location. Lossless data were obtained by adding atmospheric attenuation to the spectral data (Ref. 11). It was determined that the spectral data above 1000 Hz were free field (free from ground reflections) by comparing with data reported in Ref. 10 for flow from the conical nozzle alone.

The acoustic data on the side opposite the shielding stream ($\phi = 180^\circ$) were obtained by rotating the blocking plate about the nozzle axis while maintaining the same microphone array (Fig. 2).

Overall sound pressure level directivity patterns are presented for a constant polar radius of 5.0 meters after accounting for the effects of spherical spreading.

Perceived noise levels were calculated for a large scale nozzle by the method outlined in Ref. 12. The model data were scaled for size (to 0.69 meter diameter for a representative engine size), distance (to 335 meter flyover altitude), atmospheric attenuation for a standard day (to 288 K and 70 percent relative humidity), and frequency shifted by the appropriate scale factor (6.9).

RESULTS AND DISCUSSION

The results for the thermal acoustic shield tests are presented primarily as comparisons of sound pressure level spectra at various directivity angles and different flow conditions. A few cases of directivity patterns in terms of overall sound pressure levels and large scale perceived noise levels are also presented. The acoustic data for the conical nozzle alone are compared with those for the conical nozzle with shield flow. Based on ideal flow conditions, the total thrust for the conical nozzle with shield flow ranged from approximately 8 to 20 percent higher than that for the conical nozzle alone. The acoustic data were not adjusted for this thrust difference. If thrust differences had been included in the acoustic comparisons the conical nozzle alone spectra would have to be increased by approximately 0.3 to 0.8 dB above the measured data.

Model Scale Overall Sound Pressure Level Directivity Patterns

A comparison of directivity patterns for the model scale conical nozzle with and without shield flow is shown in Fig. 4 for two different values of subsonic conical nozzle exhaust velocity. The acoustic data are presented for a constant distance of 5.0 meters from the nozzle exit and are representative of the results obtained. The shield stream temperature and velocity, for these examples remained constant at 955 K and 219 m/sec, respectively. The results for the low conical nozzle exhaust velocity of 300 m/sec, Fig. 4(a), show very little difference in the shape of the directivity pattern and individual overall sound pressure levels either on the shielded side ($\phi = 0^\circ$) or the unshielded side ($\phi = 180^\circ$). The flow from the conical nozzle was unheated (286 K) for this case so that a maximum temperature difference for the tests described herein existed between the shield stream and conical nozzle stream. For the high velocity and total temperature case of 525 m/sec and 1101 K, respectively, shown in Fig. 4(b), the data recorded on the shielded side of the nozzle indicate a reduction in overal sound pressure levels, with little or no effect on the unshielded side. For these data, the conical nozzle stream temperature was higher than the shield stream temperature.

Comparisons of Model-Scale Spectral Data

Spectra for individual streams. - Sound pressure level spectra for the conical nozzle alone and shield stream alone are shown in Fig. 5. Data are presented for three different directivity angles (with respect to the nozzle inlet) along the sideline (Fig. 2). These data illustrate that the shield stream contributes little to the total noise level when both streams are flowing. The spectra shown for the conical nozzle alone were obtained at the lowest conical nozzle exhaust velocity of 273 m/sec so that the separation in levels, at a given frequency, represents the minimum difference that should be encountered in the experiments since the shield stream exhaust velocity was held constant throughout. The data separation shown in Fig. 5 is also typical of data at other directivity angles.

Spectra at $\phi = 0^\circ$ and 180°. - Comparisons of model-scale spectra at three different directivity angles for positions on the shielded side of the nozzle ($\phi = 0$), or aircraft flyover plane, and unshielded side ($\phi = 180^\circ$) are shown in Figs. 6 and 7. The flow conditions for the spectral data shown in Fig. 6 are the same as those for the conical nozzle low velocity OASPL plots of Fig. 4(a). The results shown in Fig. 6 indicate that with shield flow, lower high frequency sound pressure levels occur on both sides of the nozzle, compared to those of the conical nozzle alone. These results show that the shielding stream acts as more than a simple reflector, since the high frequency noise is also reduced on the unshielded side. The possibility exists that the noise reduction on the unshielded side of the nozzle was caused by leakage flow through the blocking plates. As the directivity angle increased, a larger reduction in high frequency noise occurred, which was typical at all test conditions.

The results for a high conical nozzle exhaust velocity are shown in Fig. 7. For this case the unshielded side ($\phi = 180^\circ$) shows no attenuation for directivity angles of 46° and 95° (Figs. 7(a) and (b), respectively), but attenuation does occur on the shielded side of the nozzle ($\phi = 0^\circ$). At $\theta = 139^\circ$, Fig. 7(c), attenuation occurs on both sides of the nozzle with a

pronounced reduction in high frequency levels occurring on the shielding side. The turnup in high frequency (>20 KHz) sound pressure levels is attributed to anomolous instrumentation benavior. The trend of increased high frequency noise attenuation with increased conical nozzle exhaust velocity will be shown more explicitly in a later section.

Spectral data for various conical nozzle and shield flow conditions. - Representative results for various nozzle/shield flow conditions are presented in Figs. 8 to 11. The figures present spectral data measured on the sideline in the forward quadrant ($\theta = 46^\circ$), approximately at right angles to the nozzle axis ($\theta = 95^\circ$), and the rear quadrant ($\theta = 139^\circ$) near the peak noise location. Conical nozzle flow conditions range from a low subsonic exhaust velocity (Fig. 8) to a high supersonic velocity (Fig. 11). Shield flow velocity was held constant at approximately 216 m/sec and data were obtained for three different nominal shield temperatures of 710, 830, and 930 K. The data shown are for $\phi = 0^\circ$.

General trends apparent from the data include the fact that shield flow attenuates conical nozzle high frequency sound pressure levels and that the attenuation increases with directivity angle. Also, it is apparent that, for the nozzle configuration used herein, the spectral results with shield flow are unaffected by changes in shield flow temperature over the range of shield temperatures investigated. (This was also true for the unshielded side of the nozzle). In addition, an increase in high frequency attenuation occurs with an increase in conical nozzle exhaust velocity (or decrease in velocity ratio, V_s/V_j, since shield stream velocity was held constant).

It should also be noted that for the low supersonic nozzle exhaust velocity case (Fig. 10(a)) shield flow appears to eliminate a tone from the conical nozzle alone in the forward quadrant at a directivity angle of 46°. Also, the peak levels for the tone free spectra are shifted to a higher frequency by about one 1/3-octave band. (This was also true for the unshielded side of the nozzle).

Spectral attenuation as a function of velocity ratio. - For the range of conditions covered by the experiments, the data indicated that in general, increased attenuation occurred with a decrease in the ratio of shield -to- conical nozzle exhaust velocities. These results are shown explicitly for a directivity angle of 139° in Fig. 12. The change in sound pressure level with and without shield flow is plotted as a function of frequency with velocity ratio as the parameter. Data for a constant shield temperature (942 K) only are presented since it was shown that variation in shield temperature, over the range investigated, has no effect on the sound pressure level with shield flow. Data above 20 KHz are not shown because of the occurrence of anomolous irregularities in the measurements, mentioned previously. The data in the figure show clearly that attenuation increases with frequency and the general trend, especially at high frequencies, is for an increase in attentuation with a decrease in velocity ratio. This implies that a minimum value of velocity ratio exists for a maximum attentuation. Also, at a given velocity ratio, variation in jet temperature (T_j) influences the results slightly.

Single Engine-Size Nozzle Results Inferred from Model-Scale Data

Large scale spectra. - The thermal acoustic shield model data were used to determine the noise suppression benefits at large scale in the flyover plane ($\phi = 0^\circ$) after modifying the individual spectra for size, distance and

atmospheric attenuation. A scale factor of 6.9 was used to give a large scale nozzle diameter of 0.69 meters. The sound pressure levels were increased and the frequency shifted in accordance with the scale factor. A flyover distance of 335 meters was used and attenuation due to spherical spreading and atmospheric attenuation for a standard day of 288 K and 70 percent relative humidity was accounted for

The large-scale spectra are presented in Fig. 13 for four different flow conditions. The large scale data of Fig. 13(c) were derived from the model scale data shown in Fig. 10(c). Attenuation of sound pressure levels occur above 250 Hz for all flow conditions shown at large scale.

Perceived noise levels. - The spectral plots of Fig. 13 were used to calculate large scale single engine perceived noise levels shown in Fig. 14. The figure presents the variation of flyover perceived noise level ($\phi = 0^\circ$), with and without shield flow, with distance along the flight path. Flight effects are not included. If the aircraft is at zero distance, then observers stationed on the ground at various intervals would be subjected to the perceived noise levels as indicated on the figure for the two different nozzle configurations.

Results for the subsonic conical nozzle exhaust velocity conditions, Figs. 14(a) and (b), show a decrease in perceived noise levels with shield flow for all sideline locations with the greatest effect occurring in the rear quadrant near the peak noise level location. The results for the higher velocity, Fig. 14(b), show a decrease in the peak level of about 4.5 PNdB at a directivity angle of 139°, whereas for the lower velocity condition, Fig. 14(a), a reduction of 2.5 PNdB occurs at a directivity angle of 115°. Again, the increase in attenuation with decrease in velocity ratio is evident from these results.

Results for two supersonic conical nozzle exhaust velocity conditions are presented in Figs. 14(c) and (d). For the lower exhaust velocity condition, Fig. 14(c), the variation of perceived noise level is not as great as for the other conditions shown in Fig. 14 either with or without shield flow. Attenuation of jet mixing noise in the rear quadrant ($\theta > 95^\circ$) with shield flow is still evident for this flow condition. Elimination of the tone at a directivity angle of 46° with shield flow causes a reduction in perceived noise level at this location at about 4 PNdB. (See Fig. 10(a) for model scale spectra for the same nominal flow conditions as those for Fig. 14(c)).

For the high conical nozzle exhaust velocity condition, Fig. 14(d), shield flow again attenuates the noise from the conical nozzle alone at all sideline locations with the greatest effect in the rear quadrant where the peak noise level is reduced by about 6 PNdB.

From the plots of perceived noise levels as a function of distance in Fig. 14, flyover relative noise levels (FRNL) were computed by the method described in Ref. 13. Flyover relative noise levels are analogous to effective perceived noise levels except that forward flight effects are not taken into account. The change in FRNL values between the conical nozzle with and without shield flow are given in the following table for the results shown in Fig. 14. Shield stream velocity and temperature were held constant at 219 m/sec and 940 K, respectively.

Flyover Relative Noise Levels for Conditions of Fig. 14

Conical nozzle exhaust velocity, V_j, m/sec	$\Delta FRNL = FRNL_{WS} - FRNL_{WOS}$, EPNdB
Subsonic flow	
301 (Fig. 14(a))	-1.9
575 (Fig. 14(b))	-4.2
Supersonic flow	
349 (Fig. 14(c))	-2.5
666 (Fig. 14(d))	-4.6

As shown in the table, ΔFRNL values range from -1.9 to -4.6 EPNdB over the range of flow conditions listed, with greater numerical values of ΔFRNL occurring for lower values of shield to jet velocity ratio for both the subsonic and supersonic flow regimes.

CONCLUDING REMARKS

The results of a limited exploratory experimental study show that a semi-annular thermal acoustic shield consisting of a low velocity, high temperature, gas stream partially surrounding a central jet exhibits lower noise levels than when the central jet is operated alone. The reduction in noise levels occurs at the high frequency end of the spectrum and primarily at high directivity angles (measured with respect to the nozzle inlet). Variations in shield stream temperature had no effect on the sound pressure level spectra produced by the nozzle/shield configuration used over the range of temperatures investigated. Generally, an increase in attenuation occurred with a decrease in the ratio of the shield stream to conical nozzle exhaust velocities for ratios greater than about 0.3. In terms of a relative engine-scale effective perceived noise level, reductions up to 4.6 EPNdB were calculated for the nozzle/shield configuration used.

APPENDIX A

D	diameter
FRNL	flyover relative noise level, EPNdB
M	Mach number
OASPL	overall sound pressure level, dB (re 20 $\mu N/m^2$)
PR	nozzle pressure ratio
SPL	sound pressure level, dB (re 20 $\mu N/m^2$)
T	nozzle total temperature
V	nozzle exhaust velocity
θ	directivity angle measured from nozzle inlet, degrees
ϕ	circumferential angle defined in Fig. 2, degrees

Subscripts:

j	conical nozzle stream
ls	large scale
s	shielding stream
wos	without shield flow
ws	with shield flow

REFERENCES

1. Rudnick, I., "Acoustic Transmission Through a Fluid Lamina," Acoust. Soc. Am., 17, (3), 245-253 (1946).

2. Jones, I. S. F., "Jet Noise Suppression by an Impedance Shroud," Document D1-82-0984, Boeing Scientific Research Labs., Seattle, WA (June 1970).

3. Norum, T. D., "Measured and Calculated Transmission Losses of Sound Waves Through a Helium Layer," NASA TN D-7230 (May 1973).

4. Cowan, S. J. and Crouch, R. W., "Transmission of Sound Through a Two-Dimensional Shielding Jet," AIAA Paper 73-1002 (October 1973).

5. Morris, P. J., Richarz, W., Ribner, H. S., "Reduction of Peak Jet Noise Using Jet Refraction," J. Sound Vibr., 29, 443-455 (1973).

6. Candel, S. M., Julienne, A., and Julliand, M., "Shielding and Scattering by a Jet Flow," AIAA Paper 76-545 (July 1976).

7. Ahuja, K. K. and Dosanjh, D. S., "Heated Fluid Shroud as an Acoustic Shield for Noise Reduction - An Experimental Study," AIAA Paper 77-1286 (October 1977).

8. Shivashankara, B. N. and Bhat, W. V., "Noise Characteristics of Two Parallel Jets of Unequal Flow," AIAA Paper 80-1068 (January 1980).

9. von Glahn, U. H., "Acoustic Considerations of Flight Effects on Jet Noise Suppressor Nozzles," NASA TM 81377 (January 1980).

10. Goodykoontz, J. H. and Stone, J. R., "Experimental Study of Coaxial Nozzle Exhaust Noise," AIAA Paper 79-0631 (March 1979).

11. Shields, F. D. and Bass, H. E., "Atmospheric Absorption of High Frequency Noise and Application to Fractional-Octave Bands," NASA CR-2760 (1977).

12. "Definitions and Procedures for Computing the Perceived Noise Level of Aircraft Noise," Aerospace Recommended Practice 865A, Society Automotive Engineers, Inc. (October 1964, Rev. August 1969).

13. Groesbeck, D. E. and von Glahn, U. H. "Assessment at Full Scale of Nozzle/Wing Geometry Effects on OTW Aeroacoustic Characteristics," NASA TM-79168 (June 1979).

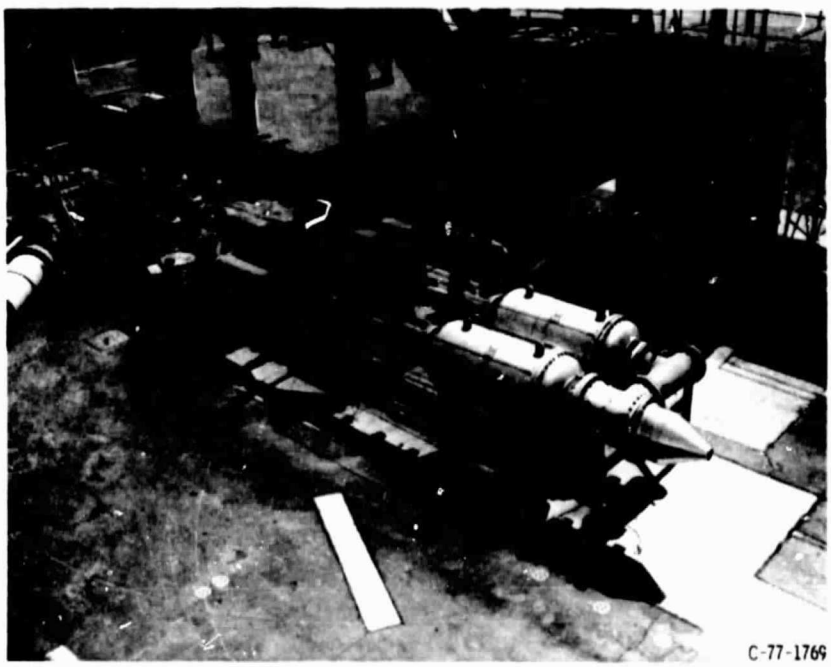

Figure 1.- Lewis hot jet acoustic facility.

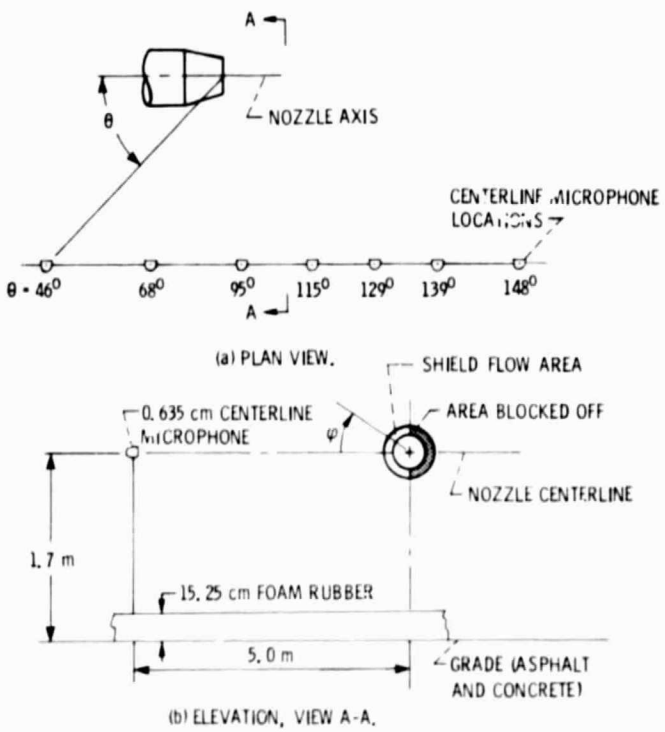

Figure 2. - Acoustic arena and microphone layout.

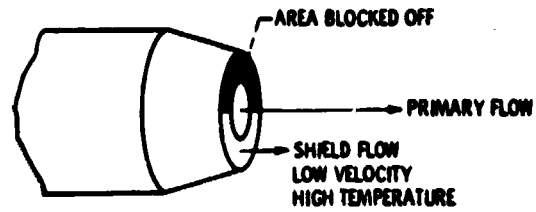

(a) PERSPECTIVE VIEW OF NOZZLE.

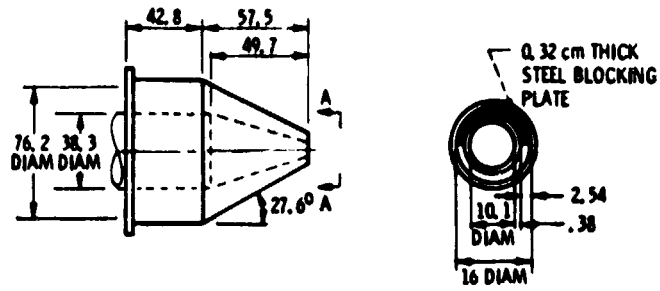

(b) NOZZLE DIMENSIONS.

ENLARGED VIEW A-A

Figure 3. - Schematic of thermal acoustic shield nozzle configuration. All dimensions in centimeters.

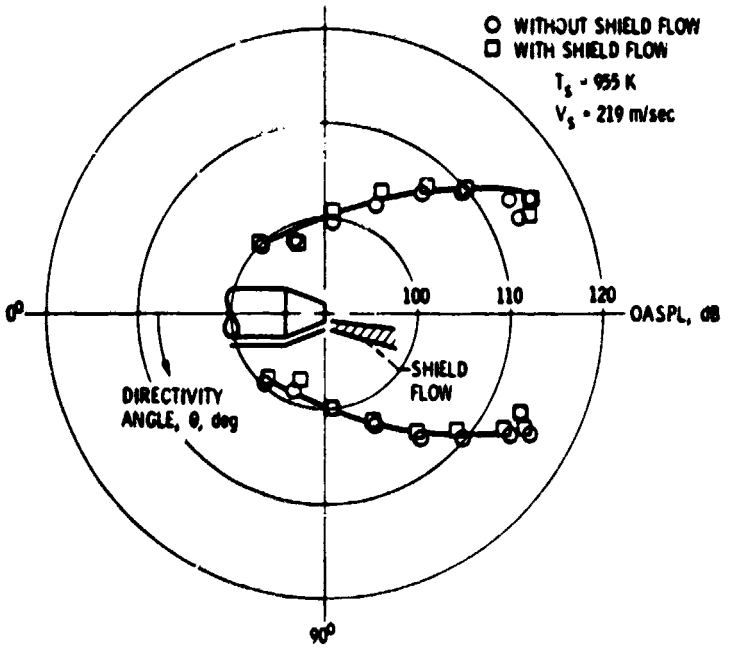

(a) LOW SUBSONIC CONICAL NOZZLE EXHAUST VELOCITY AND TOTAL TEMPERATURE. PR_j = 1.79, T_j = 286 K, V_j = 300 m/sec, M_j = 0.94.

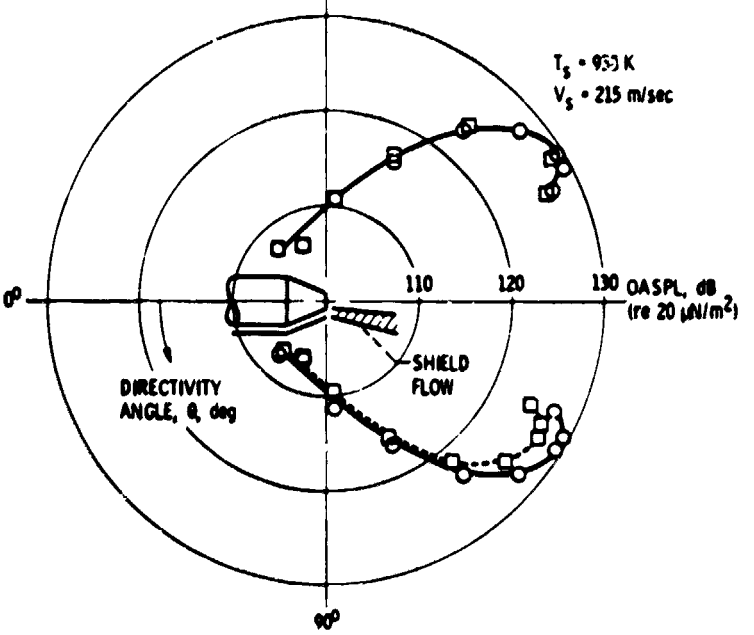

(b) HIGH SUBSONIC CONICAL NOZZLE EXHAUST VELOCITY AND TOTAL TEMPERATURE. PR_j = 1.58, T_j = 1101 K, V_j = 525 m/sec, M_j = 0.84.

Figure 4. - Effect of shield flow on conical nozzle overall sound pressure level directivity patterns. Polar radius = 5.0 m. Model scale data.

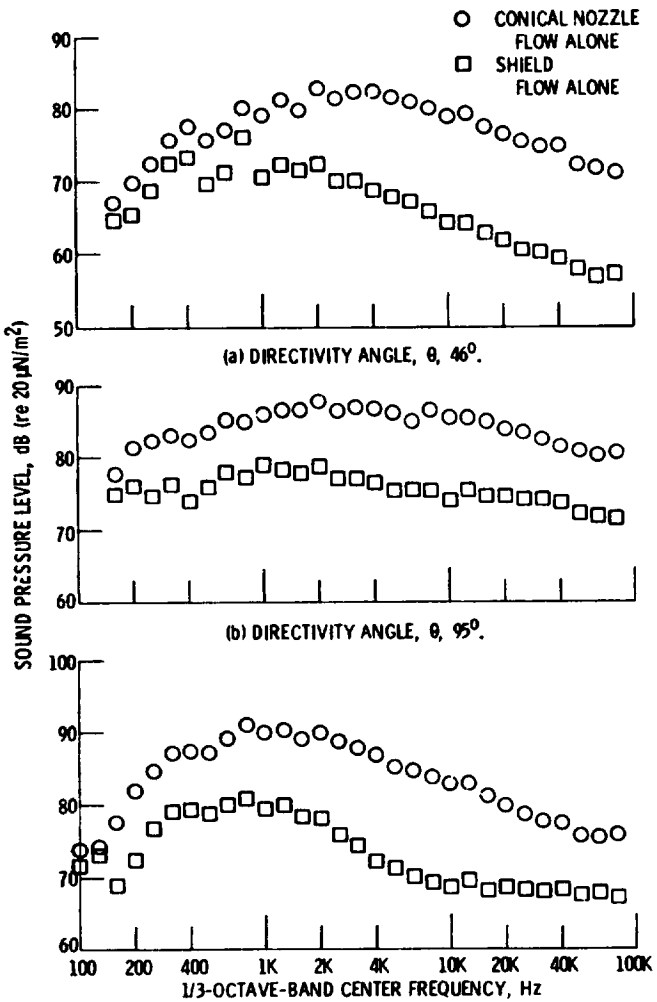

Figure 5. - Comparison of spectra for conical nozzle flow alone and shield flow alone. $PR_j = 1.60$, $T_j = 294$ K, $V_j = 273$ m/sec. $T_s = 935$ K, $V_s = 220$ m/sec. Model scale data.

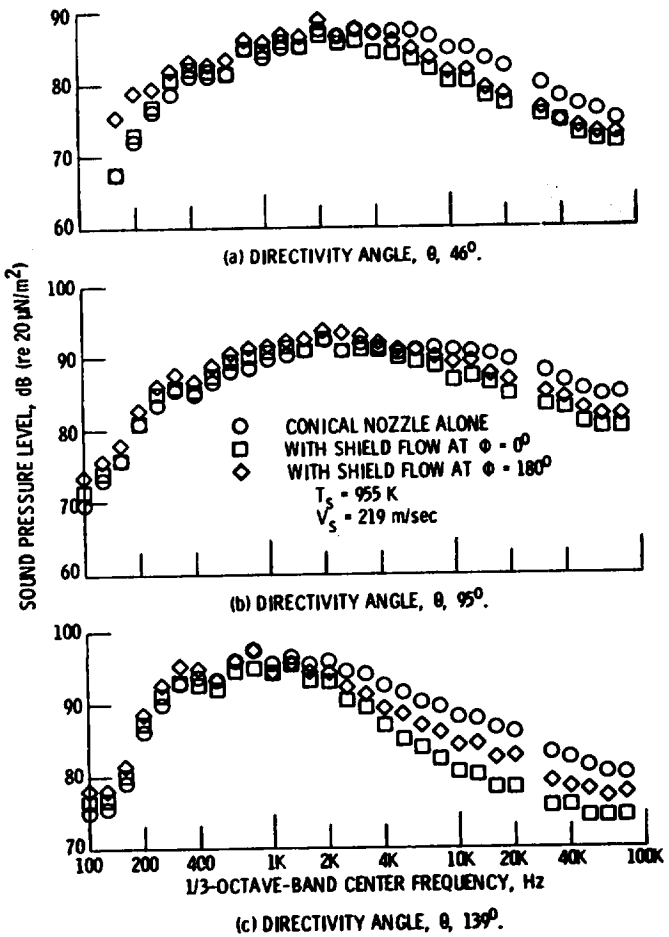

Figure 6. - Comparison of spectra at different circumferential locations for subsonic core flow. $PR_j = 1.79$, $T_j = 286$ K, $V_j = 300$ m/sec, $M_j = 0.94$. Model scale data.

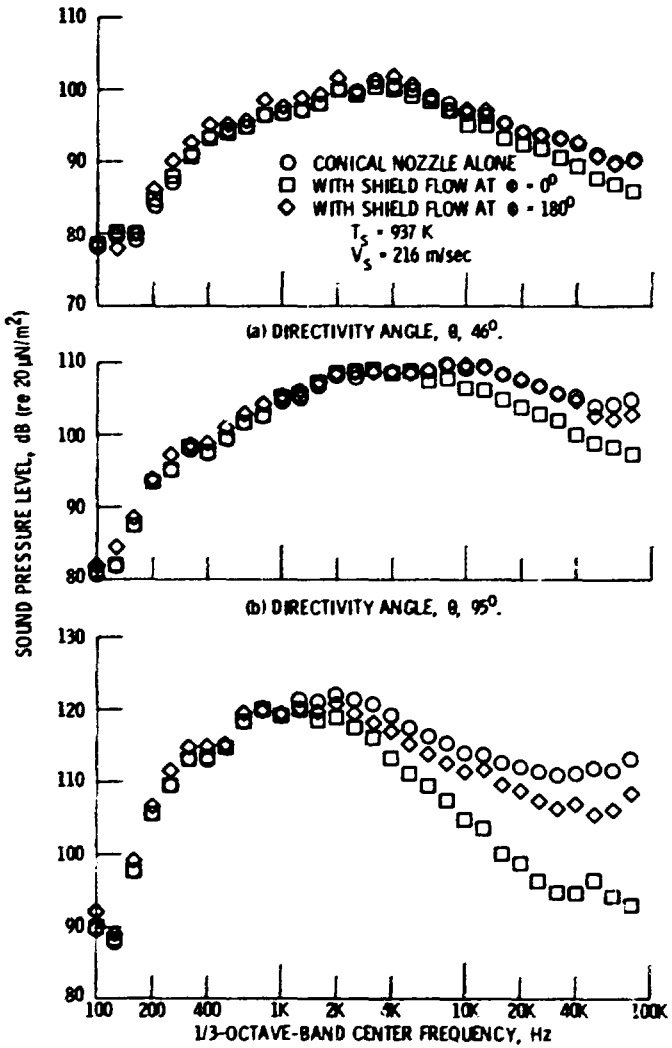

Figure 7. - Comparison of spectra at different circumferential locations for supersonic core flow. $PR_j = 2.18$, $T_j = 1095$ K, $V_j = 671$ m/sec, $M_j = 1.14$. Model scale data.

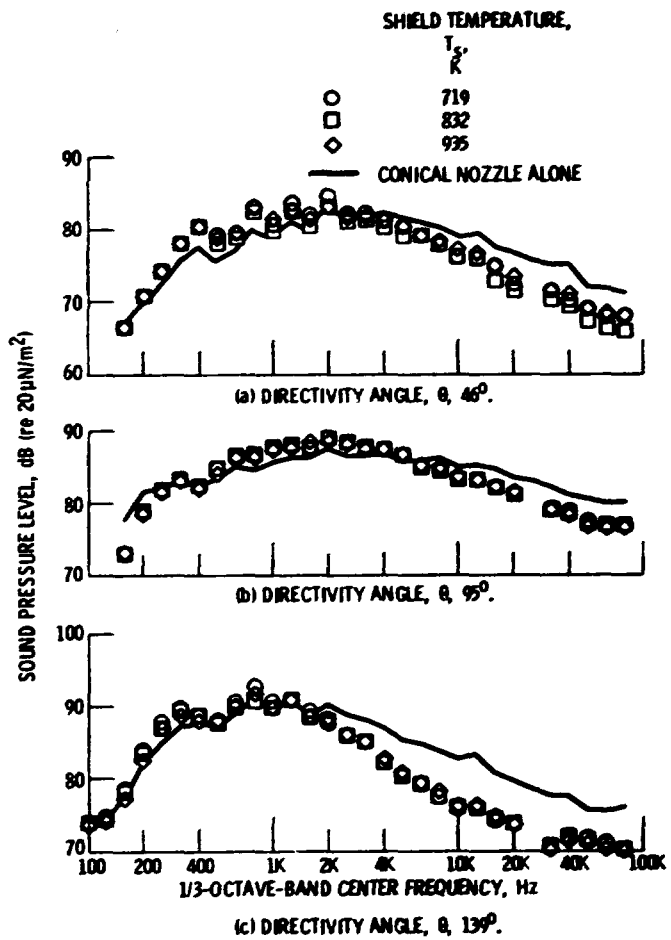

Figure 8. - Effect of shield flow on conical nozzle sound spectra at low subsonic conical nozzle exhaust velocity and total temperature. $PR_j = 1.56$, $T_j = 287$ K, $V_j = 262$ m/sec, $M_j = 0.83$. Model scale data. $V_s = 216$ m/sec.

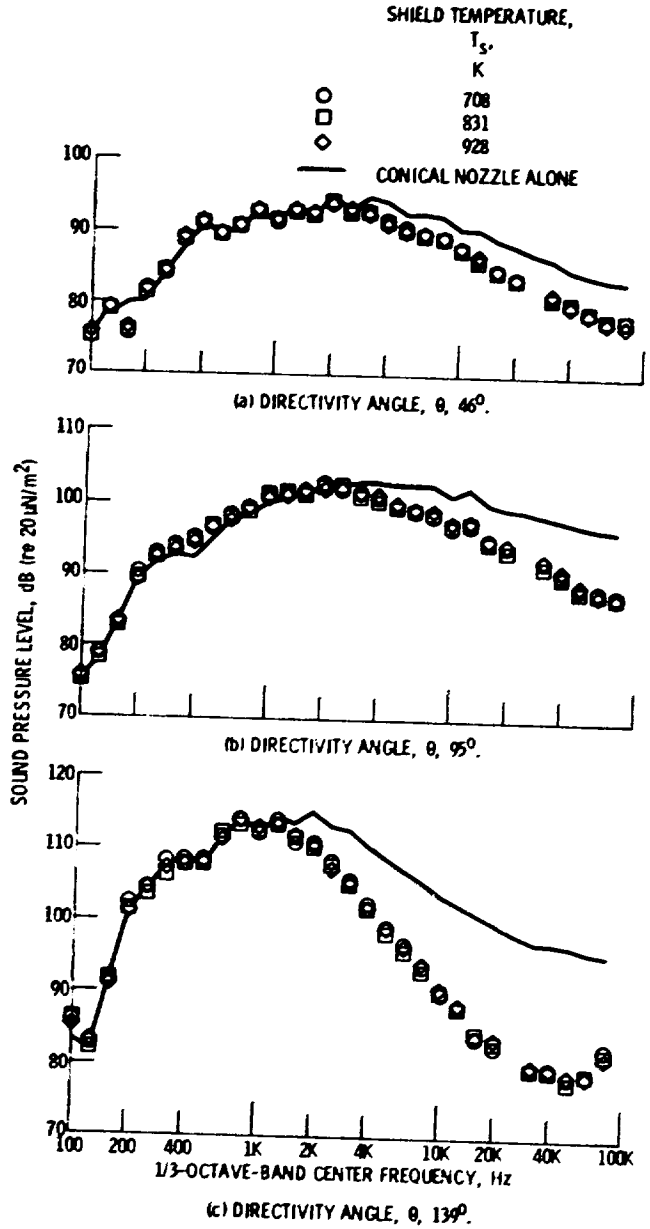

Figure 9. - Effect of shield flow on conical nozzle spectra at high subsonic conical nozzle exhaust velocity and total temperature. PR_j = 1.57, T_j = 1104 K, V_j = 521 m/sec, M_j = 0.85, V_s = 216 m/sec. Model scale data.

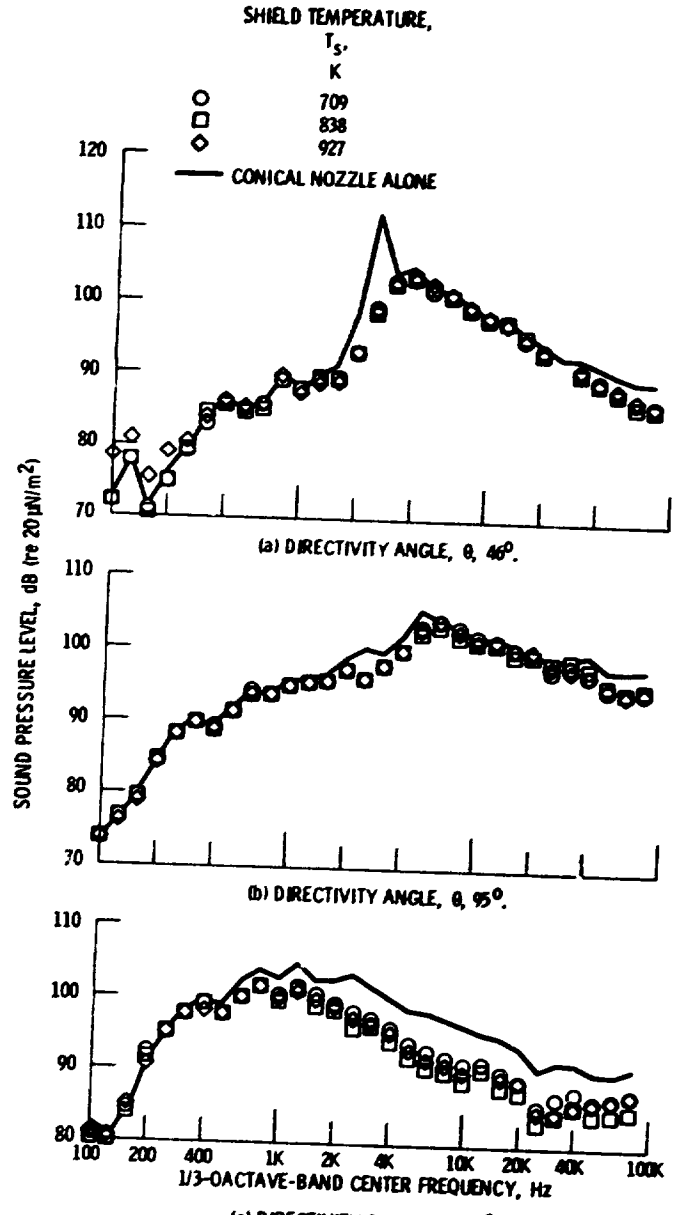

Figure 10. - Effect of shield flow on conical nozzle sound spectra at low supersonic conical nozzle exhaust velocity and total temperature. PR_j = 2.18, T_j = 292 K, V_j = 342 m/sec, M_j = 1.11. V_s = 217 m/sec. Model scale data.

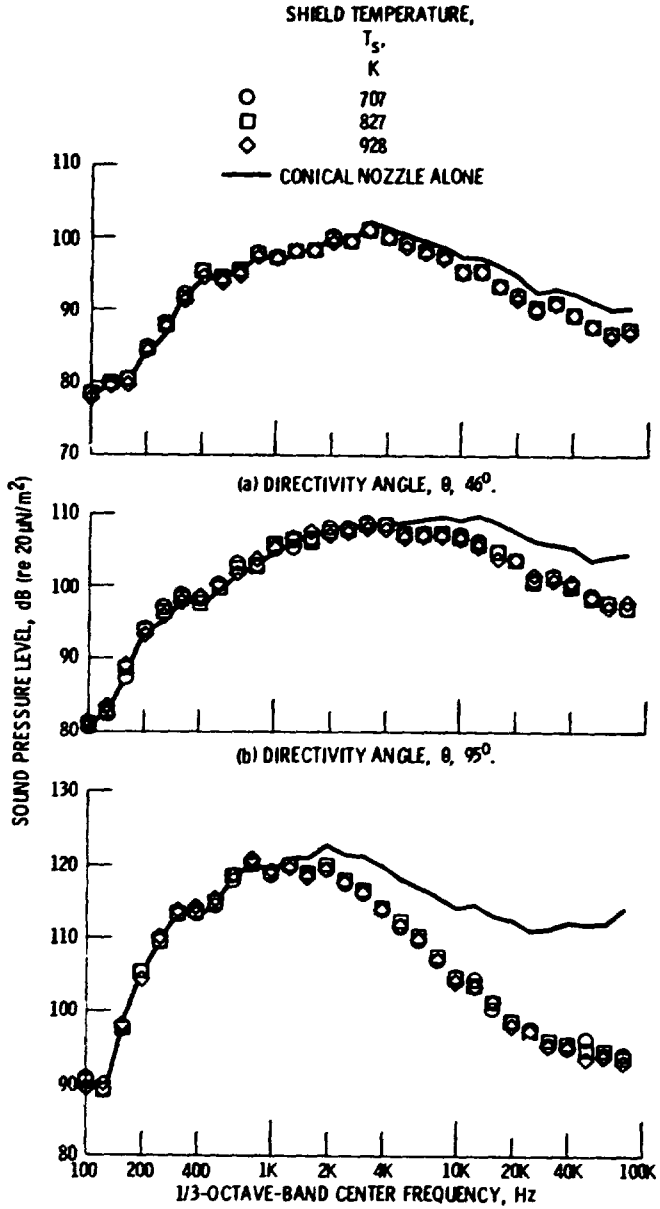

Figure 11. - Effect of shield flow on conical nozzle sound spectra at high supersonic conical nozzle exhaust velocity and total temperature. PR_j = 2.17, T_j = 1098 K, V_j = 670 m/sec, M_j = 1.14. V_s = 215 m/sec. Model scale data.

CONICAL NOZZLE NOMINAL FLOW CONDITIONS

	VELOCITY RATIO, V_s/V_j	PRESSURE RATIO, PR_j	TEMPERATURE, T_j, K	VELOCITY, V_j, m/sec
○	0.33	2.15	1098	666
□	.38	1.74	1102	575
◇	.38	2.14	810	570
△	.42	1.56	1104	518
◁	.44	1.75	809	494
▷	.50	1.55	804	440
▢	.63	2.18	306	349
◇	.73	1.80	291	301
▷	.82	1.57	294	266

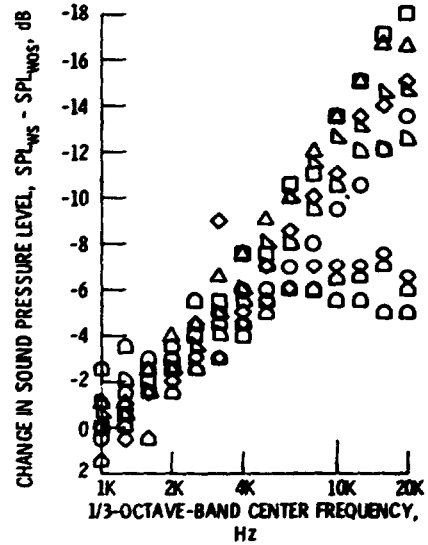

Figure 12. - Reduction in spectral sound pressure levels at θ = 139° as a result of shield flow with shield to jet velocity ratio as the parameter. Nominal shield flow conditions; T_s = 942 K, V_s = 219 m/sec. Model scale data.

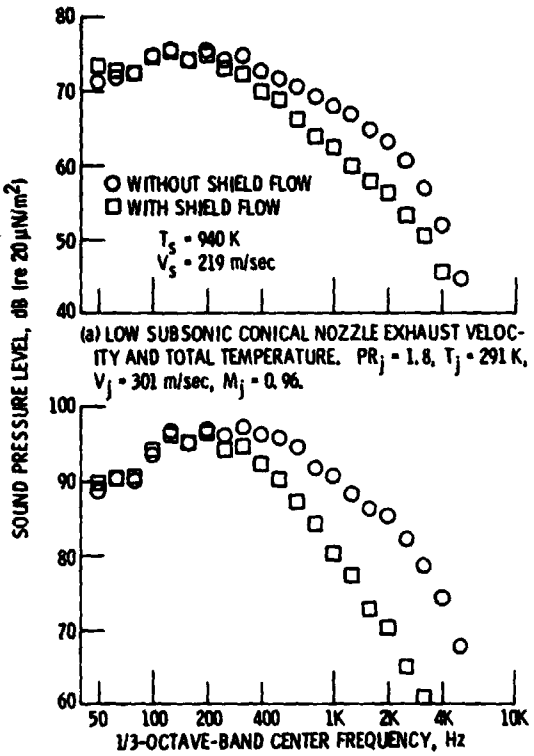

(a) LOW SUBSONIC CONICAL NOZZLE EXHAUST VELOCITY AND TOTAL TEMPERATURE. PR_j = 1.8, T_j = 291 K, V_j = 301 m/sec, M_j = 0.96.

(b) HIGH SUBSONIC CONICAL NOZZLE EXHAUST VELOCITY AND TOTAL TEMPERATURE. PR_j = 1.74, T_j = 1103 K, V_j = 575 m/sec, M_j = 0.93.

Figure 13. - Spectral data scaled to engine size for a standard day at a flyover distance of 335 meters. D_{ls} = 0.69 m, $\theta = 139^0$, ambient temperature = 288 K, relative humidity equal 70%.

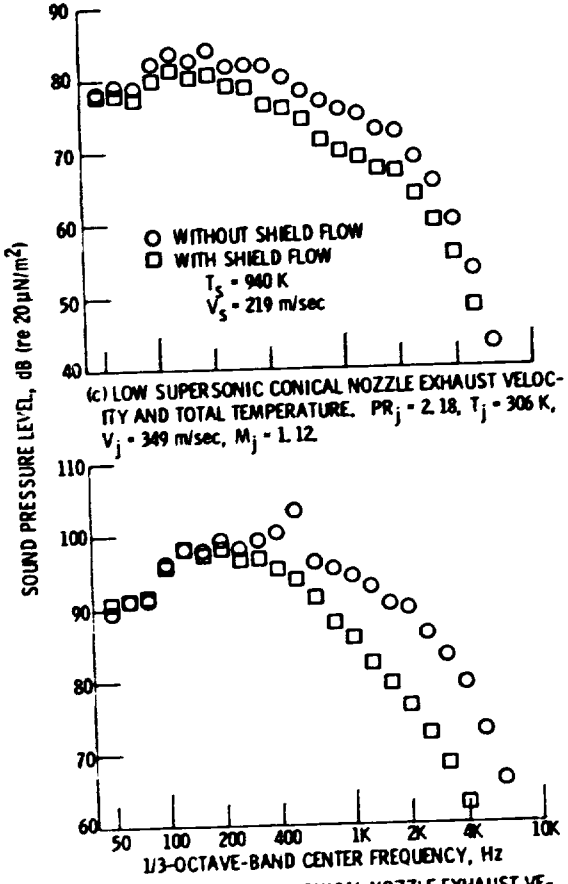

(c) LOW SUPERSONIC CONICAL NOZZLE EXHAUST VELOCITY AND TOTAL TEMPERATURE. PR_j = 2.18, T_j = 306 K, V_j = 349 m/sec, M_j = 1.12.

(d) HIGH SUPERSONIC CONICAL NOZZLE EXHAUST VELOCITY AND TOTAL TEMPERATURE. PR_j = 2.15, T_j = 1098 K, V_j = 666 m/sec, M_j = 1.11.

Figure 13. - Concluded.

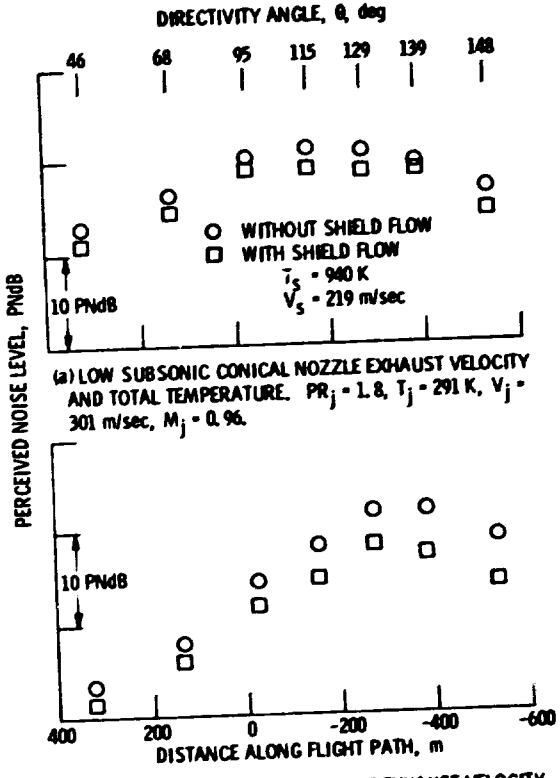

(a) LOW SUBSONIC CONICAL NOZZLE EXHAUST VELOCITY AND TOTAL TEMPERATURE. PR_j = 1.8, T_j = 291 K, V_j = 301 m/sec, M_j = 0.96.

(b) HIGH SUBSONIC CONICAL NOZZLE EXHAUST VELOCITY AND TOTAL TEMPERATURE. PR_j = 1.74, T_j = 1103 K, V_j = 575 m/sec, M_j = 0.93.

Figure 14. - Effect of shield flow on flyover perceived noise levels for a large scale conical nozzle. D_{js} = 0.69 m, flyover distance = 335 m, $\theta = 0^0$.

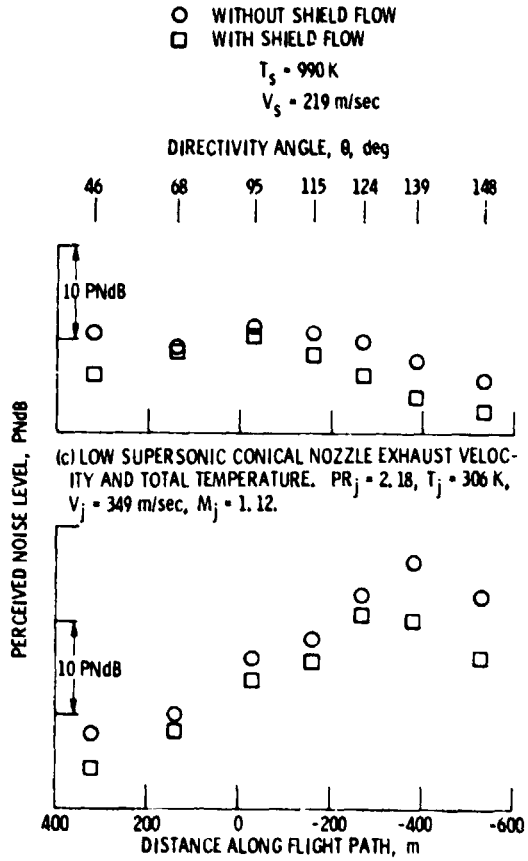

(c) LOW SUPERSONIC CONICAL NOZZLE EXHAUST VELOCITY AND TOTAL TEMPERATURE. PR_j = 2.18, T_j = 306 K, V_j = 349 m/sec, M_j = 1.12.

(d) HIGH SUPERSONIC CONICAL NOZZLE EXHAUST VELOCITY AND TOTAL TEMPERATURE. PR_j = 2.15, T_j = 1098 K, V_j = 666 m/sec, M_j = 1.11.

Figure 14. - Concluded.